Advances in the Direct Study of Carbon Burning in Massive Stars

G. Fruet, S. Courtin, M. Heine, D.G. Jenkins, P. Adsley, A. Brown, R. Canavan, W.N. Catford, E. Charon, D. Curien, et al.

Advances in the direct study of carbon burning in massive stars

G. Fruet,[1,2] S. Courtin,[1,2,3,*] M. Heine,[1,2,†] D.G. Jenkins,[4] P. Adsley,[5] A. Brown,[4] R. Canavan,[6,7] W.N. Catford,[6] E. Charon,[8] D. Curien,[1,2] S. Della Negra,[5] J. Duprat,[9] F. Hammache,[5] J. Lesrel,[5] G. Lotay,[6] A. Meyer,[5] D. Montanari,[1,2,3] L. Morris,[4] M. Moukaddam,[6] J. Nippert,[1,2] Zs. Podolyák,[6] P.H. Regan,[6,7] I. Ribaud,[5] M. Richer,[1,2] M. Rudigier,[6] R. Shearman,[6,7] N. de Séréville,[5] and C. Stodel[10]

[1]*IPHC, Université de Strasbourg, Strasbourg, F-67037, France*
[2]*CNRS, UMR7178, Strasbourg, F-67037, France*
[3]*USIAS/Université de Strasbourg, Strasbourg, F-67083, France*
[4]*University of York, York, YO10 5DD, UK*
[5]*Institut de Physique Nucléaire, CNRS/IN2P3, Université Paris-Sud, Université Paris-Saclay, 91406 Orsay Cedex, France*
[6]*Department of Physics, University of Surrey, Guildford, GU2 7XH, UK*
[7]*National Physical Laboratory, Teddington, Middlesex, TW110 LW, UK*
[8]*NIMBE, CEA, CNRS, Université Paris-Saclay, CEA Saclay F-91191 Gif sur Yvette, France*
[9]*Centre de Sciences Nucléaires et de Sciences de la Matire (CSNSM), Université Paris Sud, UMR 8609-CNRS/IN2P3, 91405 Orsay, France*
[10]*GANIL, CEA/DSM-CNRS/IN2P3, Caen, F-14076, France*

(Dated: February 21, 2020)

The ^{12}C+^{12}C fusion reaction plays a critical role in the evolution of massive stars and also strongly impacts various explosive astrophysical scenarios. The presence of resonances in this reaction at energies around and below the Coulomb barrier makes it impossible to carry out a simple extrapolation down to the Gamow window—the energy regime relevant to carbon burning in massive stars. The ^{12}C+^{12}C system forms a unique laboratory for challenging the contemporary picture of deep sub-barrier fusion (possible sub-barrier hindrance) and its interplay with nuclear structure (sub-barrier resonances). Here, we show that direct measurements of the ^{12}C+^{12}C fusion cross-section may be made into the Gamow window using an advanced particle-gamma coincidence technique. The sensitivity of this technique effectively removes ambiguities in existing measurements made with gamma ray or charged-particle detection alone. The present cross-section data span over eight orders of magnitude and support the fusion-hindrance model at deep sub-barrier energies.

INTRODUCTION

The number of fusion reactions which are critical for astrophysics is scarce. Among these, the ^{12}C+^{12}C reaction which is essential for the life cycle of massive stars, may occur at different stages of stellar evolution: explosive scenarios like Type Ia supernovae [1] which can be used as cosmological standard candles, quiescent carbon burning in the contracting core of a massive star [2, 3] at temperatures of the order of 1 GK and densities above a million g/cm^3 and possibly in superbursts of X-ray binary systems [4].

The obstacle to a reliable extrapolation of the ^{12}C+^{12}C cross-section into the astrophysically-relevant Gamow energy window is the presence of resonances in the cross section around the Coulomb barrier that continue down to the lowest collision energies accessible experimentally. This behaviour is strikingly different from the smooth variation in cross section as a function of energy typical of fusion in other heavy-ion systems.

The presence of resonances in the ^{12}C+^{12}C reaction has been hotly debated for over 60 years. The conventional wisdom is that they correspond to the formation of short-lived molecular states [5, 6], and this early suggestion has led on to far wider discussion of clustering in alpha-conjugate systems [7–12]. However, this model remains controversial: an alternate picture [13] is that the resonant behaviour is simply an artifact of the low level density of the ^{12}C+^{12}C compound system. The general trend in the reaction cross-section, masked by the presence of the individual resonances, should select sub-barrier hindrance, as widely observed in other heavy-ion systems [14, 15].

Given this controversy and the lack of a clear theoretical picture for the resonant behaviour, the main approach from the experimental side has been to perform direct measurements of the cross section to the lowest energies possible. Recently, an alternative indirect approach using the so-called "Trojan horse" method (THM) has reported strong resonances relevant to ^{12}C+^{12}C fusion corresponding to very low collision energies within and below the Gamow window for massive stars [16]. Results of this paper, *i.e.*, a substantial increase of the S-factor in the Gamow window have been discussed by A.M. Mukhamedzhanov *et al.*[17] in terms of an artifact from using an invalid plane-wave approximation. Reliable direct data as obtained in the present work are essential to normalize indirect studies, but also to shed light on the present controversy regarding indirect methods.

At the lowest collision energies, ^{12}C+^{12}C fusion mainly leads to two final systems: ^{23}Na+p and ^{20}Ne+α. This immediately suggests two techniques for determining the

cross-section of the ^{12}C+^{12}C fusion reaction, namely: (1) detection of evaporated charged particles (protons or α) and (2) detection of gamma rays from excited states of ^{23}Na and ^{20}Ne. Both techniques have been extensively employed showing consistent results at higher energies but exhibiting inconsistencies at lower energies [18–20] suggesting that systematic effects are a significant limitation [21, 22]. An approach, which provides a unique signature and which can circumvent these experimental limitations is to detect evaporated charged particles and gamma rays in coincidence. This effectively removes ambiguities, such as, those associated with protons created in reactions on target contaminants. Jiang *et al.* have pioneered this approach using a large array of high-purity germanium detectors, GAMMASPHERE, coupled to an array of annular silicon strip detectors to record the evaporated charged particles [23]. Their initial results were consistent with the results of earlier measurements using conventional techniques. However, the limitations of available beam time (a few days) and beam current (100s of pnA) did not allow them to push towards the astrophysically relevant energy region for ^{12}C+^{12}C fusion.

EXPERIMENT

Here, we report on measurements of ^{12}C fusion well into the Gamow window relevant to the most massive stars ($M_\odot \approx 25$) in the energy regime $E_{beam} = 2.2$ to 5.4 MeV (in the center-of-mass system) with the STELLA apparatus [24] for coincident gamma-particle detection. STELLA (see Figure 1) was mounted on a dedicated beam line at the Andromède accelerator facility [25] at IPN Orsay, France. The intensity of the ^{12}C($2^+/3^+$)-beam was increased from 30 pnA around the Coulomb barrrier ($E_{beam} = 6.6$ MeV) to 2 pμA for the astrophysically relevant region with data-taking periods of weeks.

STELLA comprises an ultra-high vacuum chamber ($\approx 10^{-8}$ mbar) containing a rotating target mechanism that supports large diameter (≈ 5 cm) thin (≈ 200 nm) natural carbon foils which can be rotated at up to 1000 rpm to efficiently dissipate heat from the intense ^{12}C beams and hence, prevent target deterioration. Continuous measurements of scattered beam at 45° as well as foil-thickness and homogeneity measurements after irradiation confirm that carbon buildup in the target [21, 26] is below 1% and thus negligible. Samples of material from both irradiated and non-irradiated areas of some of the target foils were analyzed by Raman spectrometry to determine possible changes in the graphite, disordered carbon and amorphous carbon signatures [27]. Single crystal graphite is characterized by a single band at 1581 cm^{-1} referred to as the G band. Amorphous carbon has a single broad and asymmetrical band centered at about 1520 cm^{-1} and disordered carbon usually shows three

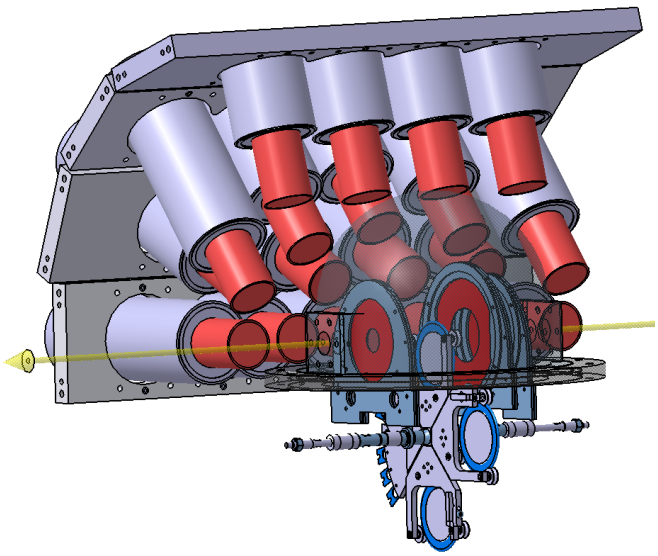

FIG. 1: 3D-rendered CAD drawing of the STELLA apparatus: The volume of the scattering chamber is shown semi-transparent in order to allow its interior to be viewed, comprising three annular silicon detectors, and a target holding/rotating mechanism. The large circular carbon target foils are shown with blue frames on their perimeter. The direction of the ^{12}C beam (from right to left in the diagram) is shown with the yellow arrow. Only half of the $LaBr_3$(Ce) gamma-ray array is depicted for clarity of presentation.

defect bands, the strongest being the D band centered at about 1350 cm^{-1} [28, 29]. The non-irradiated target foil region exhibits Raman features typical of disordered and amorphous carbon. The irradiated portions of the target foils showed nearly identical features: the ratio of the intensity of the D and G band was slightly greater (about 3 %) for the irradiated region (ID/IG = 1.28 and 1.35 for the non-irradiated and irradiated zone respectively), suggesting a marginal increase in the disordered and amorphous character of the carbon film upon heavy irradiation, but no significant change of structure of the carbon material under beam exposure.

Charged particles are detected in three annular silicon strip detectors covering 30% of 4π solid angle. For gamma-ray detection, STELLA employs an array of 36 Lanthanum Bromide ($LaBr_3$(Ce)) scintillator detectors from the UK FATIMA collaboration [30, 31], which have high energy resolution ($\approx$ 3% at 662 keV). The sub-nanosecond timing of these detectors allows tight time coincidences with charged particles for background reduction as demonstrated in Figure 2 , where the low-level internal radioactivity of the $LaBr_3$ (Ce) material represents the principal background. Such background is associated with the decay from both the primordial radionuclide ^{138}La and members of the ^{227}Ac decay chain which are incorporated in trace amounts during crystal production [32] leading to a counting rate of the order of 1-10 Bq per cm^3. However, demanding prompt-time

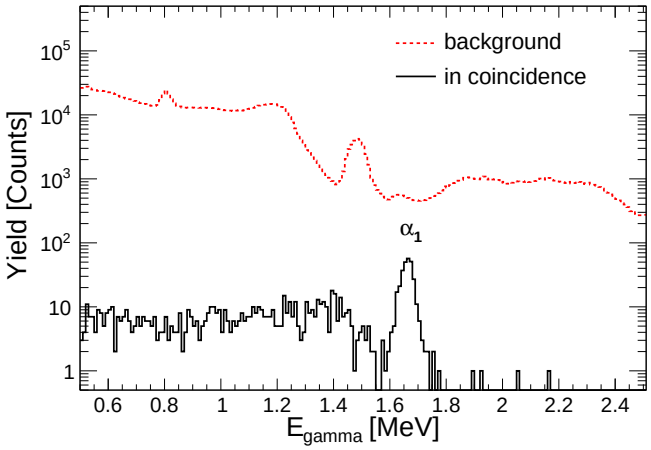

FIG. 2: Gamma-ray spectra obtained for $E_{beam} = 3.83$ MeV, without coincidence (red dashed showing the internal activity) and in coincidence (black solid) with the alpha particle channel, α_1.

coincidences with the evaporated charged particles, as presented in Figure 2, removes virtually all of this contribution to the background. The observed positions of the 789-keV and 1436-keV gamma ray peaks from the internal activity were, in fact, used to correct for the temperature-dependent gain drift of the gamma-ray detectors and their associated electronics with a precision of a few keV [24].

MEASUREMENTS

In an initial phase of measurements, data were taken using fixed targets with thicknesses varying from 20 to 70 μg/cm^2, in the relative-energy range $E_{rel} = 4.5$ to 5.5 MeV where cross-sections are typically of the order of millibarns. The initial data show good conformity with earlier measurements [18, 19, 21, 23] giving confidence in the present methodology. To study the lowest collision energies, the rotating target mechanism was employed allowing the target foils to sustain 2 pμA beam for several days without breaking.

The data from the silicon array and $LaBr_3$(Ce) array were recorded independently onto two digital data-acquisition systems and subsequently merged using correlated timestamps. The excellent timing resolution of the $LaBr_3$(Ce) as a "start" detector combined with the different effective interaction time of protons and alpha particles within the silicon substrate, automatically provides proton/alpha discrimination using the STELLA digital DAQ which is a key improvement over earlier coincidence techniques using analogue electronics [24].

For the evaluation of exclusive cross sections to the final systems ^{23}Na+p and ^{20}Ne+α, the individual reaction channels α_i and p_i to the i-th excited state were selected by requiring coincidences with the corresponding gamma-ray transitions de-exciting the states in the daughter nuclei. The principal gamma-ray transitions are those de-exciting the first excited states of ^{20}Ne (1.634 MeV) and ^{23}Na (0.440 MeV) which have corresponding gamma-ray detection efficiencies of 2% and 6%, respectively. Information on the expected branching to different alpha and proton channels from the literature [18], found to be approximately constant in the energy regime considered, has been used in order to correct for reaction channels not observed in the present study including, naturally, the ground-state branches which would not be expected to be seen using a gamma-ray coincidence technique. The systematic uncertainty from averaging amounts to 2%; a 3σ confidence interval is adopted for the extrapolation to the lowest energies beyond the available branching ratio data. Even if there were large fluctuations in the branching ratio than the 3σ interval accounted for in the extrapolation, this would be subsumed by the dominant statistical error for the lowest measured data points. For the acceptance corrections, the gamma angular distributions are known to be nearly isotropic [19, 33] while charged particle angular distributions were found to flatten out quickly with decreasing energy [18, 34].

Fusion event selection is demonstrated in Figure 3 for

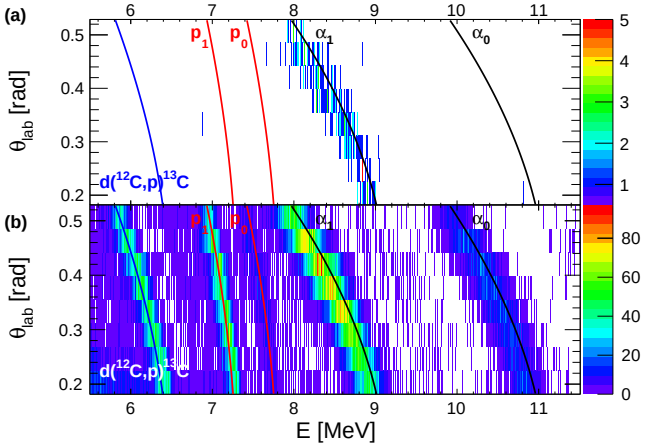

FIG. 3: Charged particle spectra from the ^{12}C+^{12}C fusion reaction as a function of lab angle for $E_{rel} = 3.77$ MeV. The bottom spectrum is the singles data without gamma-ray coincidence. The top spectrum is that for alpha-particle events in coincidence with a 1634 keV gamma ray. The locii are shown for different particle groups including protons from the contaminating d(^{12}C,p)^{13}C reaction.

$E_{rel} = 3.77$ MeV, where the deuterium contamination from d(^{12}C, p)^{13}C reactions [20] is entirely removed by selecting the γ-ray transition depopulating the first excited state in ^{20}Ne.

For the lowest energies, a statistical analysis was carried out where the background rate in the coincident energy and timing gate is determined under beam conditions. The evaporation products have a well-defined and relatively narrow time offset with respect to de-

excitation gammas, while non-correlated background was determined well outside this coincidence window applying the same particle selection-criteria but wider timing gates for higher statistical relevance. Using the likelihood estimation methods of Feldman [35], one-sigma confidence intervals were obtained around the signal for measured background and observation rates. The procedure is depicted in Figure 4 for measurements at $E_{rel} = 2.16$ MeV with three-sigma bands (dashed lines) around the nominal kinematic locus for the p_1 proton channel (solid line).

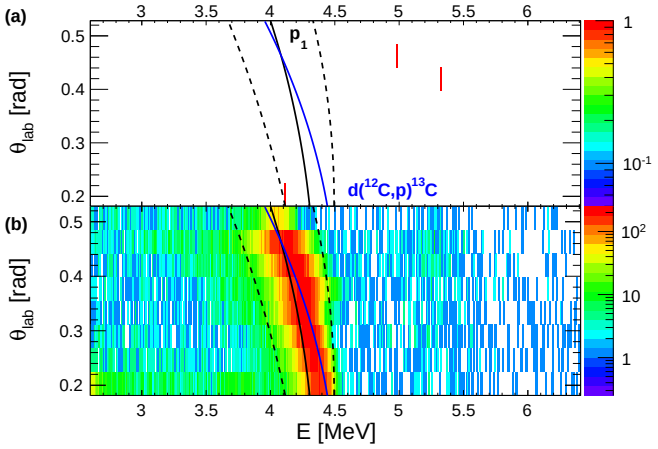

FIG. 4: Charged particle spectra from the ^{12}C+^{12}C fusion reaction as a function of lab angle for $E_{rel} = 2.16$ MeV. The bottom spectrum is the singles data without gamma-ray coincidence dominated by protons from the contaminating d(^{12}C,p)^{13}C reaction (locus labelled in blue). The top spectrum is that for proton events in coincidence with a 440 keV gamma ray. The locus is shown for the p_1 events with the dashed lines indicating 3-sigma windows on the proton energy resolution.

The carbon beam undergoes energy loss predominantly from multiple scattering in the target foils. To calculate the effective beam energy E_{eff}, the varying fusion cross section within the target was interpolated with an exponential response function:

$$\sigma(E) = \sigma_s \frac{E_s}{E} \mathrm{e}^{\left[A_0(E-E_s) - B_0 \frac{1}{E_s^{N_p-1}(N_p-1)} \left(\left(\frac{E_s}{E}\right)^{N_p-1} - 1\right)\right]},$$

where σ_s, E_s, A_0 and B_0 are free parameters and $N_p = 1.5$ [36]. In the minimization, cross-section data were matched with the response function in the area of each energy loss interval. The effective beam energy was then interpolated as the weighted mean value determined from the cross section drop within the energy-loss interval.

RESULTS

In order to display the sub-barrier cross sections over a wide energy range, data are commonly expressed in terms of the modified S-factor S^*, where the exponential decrease related to the dominant tunneling effect through the repulsive potential is removed by defining:

$$S^* = \sigma E \exp(2\pi\eta + gE)$$

where $\eta = Z_1 Z_2 e^2/\hbar\nu$ is the Sommerfeld parameter and $g = 0.122\sqrt{\mu R^3/Z_1 Z_2}$ is the form factor in ^{12}C + ^{12}C reactions derived for $l = 0$ states in a square-well model-potential [3, 37], with the reduced mass μ, the square-well radius R and the charge $Z_{1,2}$ of the nuclei. The correction $\exp(gE)$ is a form factor and needed in the present case as the interaction radius and the energy involved are so large. S-factors for ^{12}C+^{12}C fusion corresponding to alpha evaporation are presented in Figure 5, and with proton evaporation in Figure 6 as a function of the relative energy E_{rel}, and compared to previous measurements. Two extrapolations are presented based on a smoothed out average cross-section (blue dash-dotted line) [38] and a phenomenological hindrance model (red dotted line) [36]. In the supplementary material, an excerpt of the energy region of the hindrance phenomenon [39] is provided.

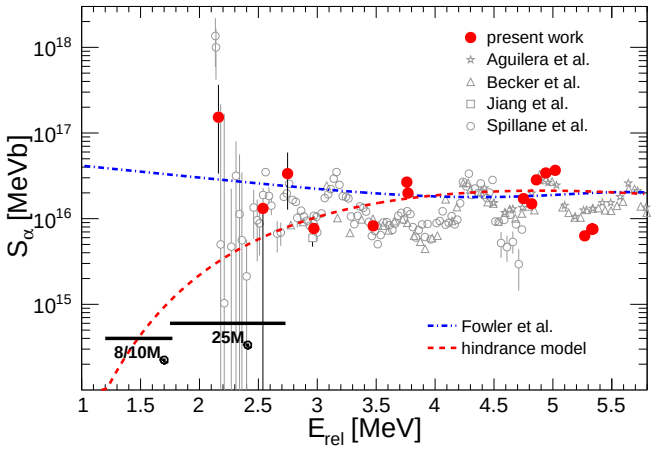

FIG. 5: S-factor measurements for the ^{12}C+^{12}C fusion reaction as a function of E_{rel} for the final system ^{20}Ne+α. The present data, at the effective beam energy (see text for details), are presented as red circles and compared to earlier measurements (grey symbols) [18, 19, 21, 23]. The blue dash-dotted line is a standard extrapolation of the data [38], while the red dashed line corresponds to a sub-barrier hindrance model [36]. The Gamow windows for 8/10M$_\odot$ and 25M$_\odot$ correspond to stellar temperatures of 0.5GK and 0.9GK, respectively.

The present data do not require any reaction model for their interpretation (such as in the recent THM experiment) and span the region from the Coulomb barrier down to the upper end of the Gamow window with significantly improved accuracy. They are in good agreement with the data reported by Jiang *et al.* [23] using similar techniques, and with the re-normalized THM data [17]. In the intermediate energy range at $E_{rel} = 3.8$ MeV, a

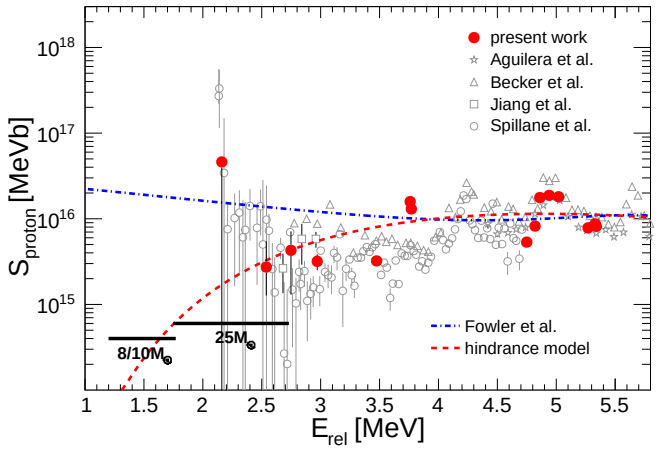

FIG. 6: S-factor measurements in similar context as Figure 5, but for the final system ^{23}Na+p.

more prominent resonance is observed compared to previous measurements [19, 20].

The data for the proton-evaporation channel strongly supports the extrapolation based on the hindrance model with an excellent match well below the predicted S-factor maximum around 3 to 4 MeV [39]; the lowest data point being less discriminating since it corresponds to a one-sigma upper limit. The data for the alpha-evaporation channel broadly support the hindrance model and also provide evidence for the resonance at $E_{rel} = 2.14$ MeV reported by Spillane *et al.* [19], albeit with a reduced resonance strength.

Corrections from electron screening effects can lead to an enhancement of the reaction rate determined in the laboratory for its application in the astrophysical site. The nuclei in the target material are shielded by the surrounding electrons, which effectively lowers the Coulomb well as compared to a bare nucleus. Therefore an enhanced cross section is detected. This screening effect on the S-factor is most efficient at the lowest beam energy and in the present study it was estimated based on the Rutherford-Bohr model of the atom [40], where the shielding potential is defined by the Coulomb field at the innermost electron ring. The effect for ^{12}C+ ^{12}C collisions considered here is found to be less than 3%, which is included in the systematic uncertainty ($\leq 17\%$). Note that in experimental studies of reactions with light projectiles ($Z \leq 3$) a systematically higher enhancement was observed [41], while a more complementary analysis procedure [42] could extract screening potentials as predicted with the atom-physics model.

DISCUSSION

The measurement with the STELLA experimental station has allowed the extraction of reliable excitation functions for the ^{12}C+^{12}C fusion reaction over eight orders of magnitude in cross section. It was possible to probe well below the Coulomb barrier into the Gamow window for massive stars using the gamma-particle coincidence technique. Key to these advances were the excellent timing properties of the $LaBr_3$ detectors, the novel self-supporting rotating target system, and the dedicated low-noise particle detector system.

The results identify three distinct regimes in the sub-Coulomb range: (i). The moderate sub-barrier regime above $E_{rel} = 4.5$ MeV—where it has been possible to unambiguously validate our experimental concept by accurately measuring the excitation function of the ^{12}C+^{12}C fusion reaction, (ii). The deep-sub-barrier regime from $E_{rel} = 2.5$ to 4 MeV—where the Fowler standard extrapolation systematically overestimates the results and where hindrance is observed. (iii). The 25 solar masses Gamow window—below $E_{rel} = 2.5$ MeV—where the S-factor rises up and may indicate a change in the fusion mechanism. The latter may reveal either the presence of a resonance and/or may be interpreted as the consequence of the low level density of states in ^{24}Mg at these excitation energies [13]. The observation of hindrance behaviour, as the dominant mechanism with molecular doorway resonances built on it, is a plausible explanation but this would artificially split the fusion process into two processes. A simpler explanation could be that the large spacing of narrow levels in the even-even ^{24}Mg nucleus, accessed via the collision of the two identical bosons (^{12}C nuclei) has a limited phase space (akin to Pauli repulsion), where only a few final states are available for the fusion process to occur.

The fusion-hindrance behavior suggested by the present work would serve to raise the carbon-burning ignition temperature since it shifts the equilibrium related to heat generation by ^{12}C fusion, and that of the temperature and density-dependent heat transport by neutrinos [43]. As a consequence, the lowest fusion energy explored in the present work would be well inside the Gamow window for a star of 25 solar masses. In addition, neutron-seed generation should be affected by the observed fusion trend [44, 45]. Our results will be applied to further investigations of the advanced burning phases in massive stars, to improve our understanding of their end-points and the flux of neutrinos produced as well as providing information on the probability of type Ia supernovae [46, 47].

ACKNOWLEDGMENTS

We thank M. Lorrigiola (LNL, Padova, Italy) and G. Frémont (GANIL, Caen, France) for the excellent preparation of the reaction targets. The construction of STELLA was funded by the University of Strasbourg IdEX program and CNRS Strasbourg. The An-

dromède facility (ANR-10-EQPX- 23) was funded by the program for future investment, EQUIPEX. This work was also partially supported by the UK Science and Technology Facility Council via grants ST/L005743/1, ST/P003885/1 and ST/P005314/1. P.H. Regan and R. Shearman acknowledge support from the UK Department for Business, Energy and Industrial Strategy (BEIS) via funding for the UK National Measurement System. D. Jenkins and S. Courtin acknowledge support from their Fellowships in the University of Strasbourg Institute of Advanced Study (USIAS).

* Contact: Sandrine.Courtin@iphc.cnrs.fr
† E-mail: Marcel.Heine@iphc.cnrs.fr

[1] S.E. Woosley, A. Heger, and T.A. Weaver, Rev Mod Phys **74**, 1015 (2002).
[2] H. Reeves and E.E. Salpeter, Phys Rev **116**, 1505 (1959).
[3] C.E. Rolfs and W.S. Rodney, *Cauldrons in the Cosmos* (Univ of Chicago Press, 1988), 1st ed.
[4] A. Cumming and L. Bildsten, Astrophys J **559**, L127 (2001).
[5] D.A. Bromley, J.A. Kuehner and E. Almqvist, Phys Rev Lett **4**, 365 (1960).
[6] K.A. Erb, R.R. Bettsand, S.K. Korotkyand, M.M. Hindiand, P.P. Tungand, M.W. Sachsand, S.J. Willett, and D.A. Bromley, Phys Rev C **22**, 22 (1980).
[7] M. Freer, H. Horiuchi, Y. Kanada-Enyo, D. Lee and U.-G. Meißner, Rev Mod Phys **90**, 035004 (2018).
[8] J.-P. Ebran, E. Khan, T. Nikšić, and D. Vretenar, Phys Rev C **90**, 054329 (2014).
[9] Y. Kanada-Enyo, Prog Theor Phys **117**, 655 (2007).
[10] E. Epelbaum, H. Krebs, T.-A. Lähde, D. Lee, and U.-G. Meißner, Phys Rev Lett **109**, 252501 (2012).
[11] M. Kimura and Y. Chiba, J Phys Conf Ser **569**, 012005 (2014).
[12] A. Diaz-Torres and M. Wiescher, Phys Rev C **97**, 055802 (2018).
[13] C.L. Jiang, B.B. Back, H. Esbensen, R.V.F. Janssens, K.E. Rehm, and R.J. Charity, Phys Rev Lett **110**, 072701 (2013).
[14] C.L. Jiang *et al.*, Phys Rev Lett **89**, 052701 (2002).
[15] B.B. Back, H. Esbensen, C.L. Jiang, and K.E. Rehm, Rev Mod Phys **86**, 317 (2014).
[16] A. Tumino *et al.*, Nature **557**, 687 (2018).
[17] A.M. Mukhamedzhanov, D.Y. Pang, and A.S. Kadyrov, Phys Rev C **99**, 064618 (2019).
[18] H.W. Becker, K.U. Kettner, C. Rolfs, and H.P. Trautvetter, Z Phys A **303**, 305 (1981).
[19] T. Spillane *et al.*, Phys Rev Lett **98**, 122501 (2007).
[20] J. Zickefoose *et al.*, Phys Rev C **97**, 065806 (2018).
[21] E.F. Aguilera, P. Rosales, E. Martinez-Quiroz, G. Murillo and M.C. Fernández, Nucl Instrum Methods B **244**, 427 (2006).
[22] C.L. Jiang *et al.*, Nucl Instrum Methods A **682**, 12 (2012).
[23] C.L. Jiang *et al.*, Phys Rev C **97**, 012801(R) (2018).
[24] M. Heine *et al.*, Nucl Instrum Methods A **903**, 1 (2018).
[25] S. Della-Negra, Innovation Rev **93**, 38 (2016).
[26] M.J.F. Healy, Nucl Instrum Methods B **129**, 130 (1997).
[27] A. Ferrari and J. Robertson, Phys Rev B **61**, 14095 (2000).
[28] A. Sadezky, H. Muckenhuber, H. Grothe, R. Niessner, and U. Pöschl, Carbon **43**, 1731 (2005).
[29] E. Charon, J.N. Rouzaud, and J. Aleon, Carbon **66**, 178 (2014).
[30] O.J. Roberts, A.M. Bruce, P.H. Regan, Z. Podolyák, C.M. Townsley, J.F. Smith, K.F. Mulholland and A. Smith, Nucl Instrum Methods A **748**, 91 (2014).
[31] P.H. Regan, Radiat Phys Chem **116**, 38 (2015).
[32] F.G.A. Quarati, I.V. Khodyuk, C.W.E. van Eijk, P. Quarati, and Dorenbos, Nucl Instrum Methods A **683**, 46 (2012).
[33] K.U. Kettner, H. Lorenz-Wirzba and C. Rolls, Z Phys A **298**, 65 (1980).
[34] M.G. Mazarakis and W.E. Stephens, Phys Rev C **7**, 1280 (1973).
[35] G.J. Feldman and R.D. Cousins, Phys Rev D **57**, 3873 (1998).
[36] C.L. Jiang, K.E. Rehm, B.B. Back, and R.V.F. Janssens, Phys Rev C **79**, 044601 (2009).
[37] J.R. Patterson, H. Winkler, and C.S. Zaidins, Astrophys J **157**, 367 (1969).
[38] W.-A. Fowler, G.-R. Caughlan and B.-A. Zimmerman, Annu Rev Astron Astrophys **13**, 69 (1975).
[39] C.L. Jiang, K.E. Rehm, B.B. Back, and R.V.F. Janssens, Phys Rev C **75**, 015803 (2007).
[40] H.J. Assenbaum, K. Langanke, and C. Rolfs, Z Phys A **327**, 461 (1987).
[41] G. Fiorentini, R.W. Kavanagh, and C. Rolfs, Z Phys A **350**, 289 (1995).
[42] F.C. Barker, Nucl Phys A **707**, 277 (2002).
[43] M. E. Bennett *et al.*, Mon Not R Astron Soc **420**, 3047 (2012).
[44] M. Pignatari, R. Hirschi, M. Wiescher, R. Gallino, M. Bennett, M. Beard, C. Fryer, F. Herwig, G. Rockefeller, and F.X. Timmes, Astrophys J **762**, 31 (2013).
[45] L.R. Gasques, E.F. Brown, A. Chieffi, C.L. Jiang, M. Limongi, C. Rolfs, M. Wiescher and D.G. Yakovlev, Phys Rev C **76**, 035802 (2007).
[46] O. Straniero, L. Piersanti and S. Cristallo, J Phys Conf Ser **665**, 012008 (2016).
[47] M. Limongi and A. Chieffi, Astrophys J **647**, 483 (2006).